ARTICLE

OBC
www.rsc.org/obc

# Conformational analysis of oleandomycin and its 8-methylene-9-oxime derivative by NMR and molecular modelling†

**Predrag Novak,*[a] Zrinka Banić Tomišić,*[a] Predrag Tepeš,[a] Gorjana Lazarevski,[a] Janez Plavec[b] and Gordana Turkalj[a]**

[a] *PLIVA–RESEARCH INSTITUTE Ltd., Prilaz baruna Filipovića 29, HR-10000, Zagreb, Croatia. E-mail: predrag.novak@pliva.hr; E-mail: zrinka.banic-tomisic@pliva.hr*

[b] *National Institute of Chemistry, Hajdrihova 19, SI-1115Ljubljana, Slovenia*

***Received 10th August 2004, Accepted 12th October 2004***
***First published as an Advance Article on the web 15th November 2004***

Conformations of the 14-membered macrolide antibiotic oleandomycin and its 8-methylene-9-oxime derivative were determined in various solvents. The experimental NMR data—coupling constants and NOE contacts—were compared with the results of molecular modelling—molecular mechanics calculations and molecular dynamics simulations. The conformational changes, on the right-hand side of the 14-membered ring, affected mostly the $^3J_{H2,H3}$ values and NOE crosspeaks H3 or H4 to H11. Oleandomycin was found to be present predominantly in the C3–C5 folded-in conformations in DMSO-$d_6$ solution, whereas in buffered $D_2O$, acetone-$d_6$ and $CDCl_3$, there was a mixture of folded-in and folded-out conformational families. The predominant conformation of the 8-methylene-oleandomycin-9-oxime derivative in solution was a folded-out one although different amounts of folded-in conformation were also present depending on the solvent. Oleandrose and desosamine sugar moieties adopted the usual and expected chair conformation. The conformation around the glycosidic bonds, governing the relative orientation of sugars *vs*. the lactone ring, showed a certain flexibility within two conformationally close families. We believe that by combining the experimental NMR data and the molecular modelling techniques, as reported in this paper, we have made significant progress in understanding the conformational behaviour and properties of macrolides. Our belief is based on our own current studies on oleandomycins as well as on the previously reported results and best practices concerning other macrolides. A rational for macrolide conformational studies and advances in methodology has been suggested accordingly.

## Introduction

Oleandomycin[1] **1** (Scheme 1) is a macrolide antibiotic composed of a polyfunctionalized 14-membered ring with oleandrose and desosamine sugar units. The exocyclic epoxide at C8 of **1** is taken to be a unique feature, without equal in any other known polyoxo macrolide. Reductive deoxygenation of C8 epoxide generated 8-methylene oleandomycin which, after treatment with hydroxylamine, gave an 8-methylene-9-oxime derivative[2] **2** (Scheme 1). A literature search has shown a lack of information concerning the conformational characteristics of oleandomycin and oleandomycin-like compounds except for four X-ray structures,[3–6] three of which (**1a**,[3] **2**[6] and **3**,[5] Scheme 1) are available through the Cambridge Structural Database[7] (CSD). The conformational behaviour of the related macrolide antibiotics such as erythromycin A, roxithromycin, clarithromycin, and azithromycin has been studied intensively[8–15] by NMR and molecular modelling methods and by single-crystal X-ray analysis. Recently, data on the 3D structure of macrolide–ribosome complexes[16–17] have once again demonstrated the importance of conformation and shape of the molecule with respect to its biological activity. Conformational analysis therefore plays an important role in the rational design of molecules with an improved biological profile.

Conformational studies on other macrolides[8–15] have demonstrated the existence of two major conformational families: folded-out and folded-in, referring to the outward and inward folding of the ring fragment C3–C5 (Scheme 1). The folded-out conformers have larger homonuclear $^3J_{H2,H3}$ values (~10 Hz), larger torsion angles between atoms H2 and H3 (~±180 °) and exhibit a close space approach of protons H4 and H11, giving rise to nuclear Overhauser enhancement (NOE) crosspeaks. Much lower $^3J_{H2,H3}$ values (~2–3 Hz), lower torsion angles (~100°) and a close space approach of atoms H3 and H11

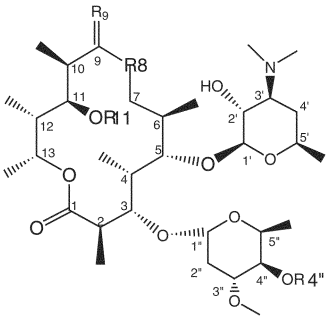


| Compound | R8 | R9 | R11, R4" | CSD[7] refcode |
|---|---|---|---|---|
| **1** |  | O | H | — |
| **1a** |  | O |  | BBOLEA[3] |
| **2** |  | NOH | H | ZATPAL[6] |
| **3** |  | NOH | H | LIDBIJ[5] |

**1** oleandomycin
**1a** 11-4"-bis(O-(p-bromobenzoyl))oleandomycin
**2** 8-methyleneoleandomycin-9-oxime
**3** 8(S)-methyloleandomycin-9-oxime

**Scheme 1** Studied compounds.

† Electronic supplementary information (ESI) available: $^1H$ and $^{13}C$ NMR data (DMSO-$d_6$, acetone-$d_6$, $D_2O$ buffer). See http://www.rsc.org/suppdata/ob/b4/b412294a/

DOI: 10.1039/b412294a

**Table 1** Experimental vicinal proton–proton coupling constants $^3J_{H,H}$/Hz for the macrocycle of compounds **1** and **2** in different solvents

| | **1** | | | | **2** | | | |
|---|---|---|---|---|---|---|---|---|
| Protons | $D_2O$ | DMSO-$d_6$ | Acetone-$d_6$ | $CDCl_3$ | $D_2O$ | DMSO-$d_6$ | Acetone-$d_6$ | $CDCl_3$ |
| H2,H3 | 7.3 | 3.9 | 6.5 | 8.4 | 9.4 | 8.0 | 7.0 | 7.9 |
| H3,H4 | 1.5 | 1.5 | 1.4 | [a] | 1.3 | 1.0 | 1.6 | 1.0 |
| H4,H5 | 7.4 | [b] | 7.1 | 7.2 | 10.2 | 10.3 | 9.8 | 10.7 |
| H5,H6 | 1.7 | [a] | 1.9 | 2.1 | [a] | [a] | 1.2 | [a] |
| H6,H7a | [a] | [a] | [a] | [a] | [a] | [a] | [a] | [a] |
| H6,H7b | [b] | [b] | 10.1 | 9.6 | 9.8 | 9.8 | [b] | 10.3 |
| H10,H11 | 1.5 | 2.1 | 2.0 | 1.5 | 1.5 | 1.5 | 1.6 | 1.5 |
| H11,H12 | 9.8 | 9.5 | 8.8 | 10.5 | 10.3 | [b] | [b] | 10.1 |
| H12,H13 | 1.4 | 2.0 | 1.8 | 1.3 | 1.1 | 1.0 | 1.3 | 1.2 |
| H1′,H2′ | 7.0 | 7.3 | 7.2 | 7.2 | 7.0 | 7.2 | 7.2 | 7.1 |
| H2′,H3′ | [b] | 10.1 | 10.2 | 10.2 | 10.2 | 10.2 | 10.1 | 10.3 |
| H3′,H4a | 4.1 | [b] | 3.9 | 3.8 | 4.1 | 3.8 | 4.0 | 3.8 |
| H3′,H4b | [b] | [b] | [b] | [b] | [b] | [b] | [b] | 9.8 |
| H4′a,H5′ | 1.9 | 1.8 | 1.9 | [b] | 1.9 | 2.0 | 2.1 | 1.9 |
| H4′b,H5′ | [b] | 10.7 | 10.9 | [b] | 9.3 | 10.8 | [b] | 10.9 |
| H1″,H2″a | 1.2 | 1.2 | 1.4 | 1.4 | 1.5 | 1.4 | 1.4 | 1.3 |
| H1″,H2″b | 3.1 | [b] | 3.7 | 3.3 | 3.4 | 3.9 | 3.9 | 3.8 |
| H2″a,H3″ | 4.9 | 4.7 | 4.7 | 4.5 | 4.7 | 4.5 | 4.7 | 4.4 |
| H2″b,H3″ | [b] | 11.7 | 11.6 | 11.6 | [b] | [b] | 11.6 | 12.7 |
| H3″,H4″ | 9.5 | 9.3 | 9.0 | 9.0 | 9.3 | 9.0 | 9.1 | 9.1 |
| H4″,H5″ | 9.4 | 9.3 | 9.3 | 9.0 | 9.4 | 9.2 | 9.2 | 9.3 |

[a] Unresolved. [b] Signal overlap.

with the corresponding NOE crosspeaks are characteristic of the folded-in conformers.[8,11,14]

To assess the conformational properties of oleandomycin-like compounds in solution we carried out a detailed NMR study of oleandomycin **1** (Scheme 1) and its derivative 8-methylene-oleandomycin-9-oxime **2** (Scheme 1).

Complete unambiguous assignment of $^1H$ and $^{13}C$ NMR spectra was necessary before performing conformational analysis.[2,18]. The information about the torsion angles, defining the conformation, was obtained from the vicinal spin–spin coupling constant data and the information about proton–proton spatial proximity was derived from the NOE data. Variable solvent and temperature experiments were performed to check the conformational flexibility and stability of the investigated molecules. Crystal structure conformations[3,5,6] being unable to account for all the NMR data of **1** and **2**, molecular mechanics calculations and unconstrained molecular dynamics simulations were applied for modelling the solution state conformations. The calculated molecular dynamics trajectories were searched for the conformers consistent with the experimental NMR data. The modelled solution state conformations were compared to the solid-state conformations retrieved from the Cambridge Structural Database[7] and to the conformations of related macrolides in corresponding solvents.

## Results and discussion

### Assignments

The complete $^1H$ and $^{13}C$ atom reassignments were made on the basis of the combined use of several one- ($^1H$ and APT sequences) and two-dimensional homo- and heteronuclear experiments (COSY, HSQC and HMBC sequences). The $^1H$ and $^{13}C$ chemical shift values in $CDCl_3$ were in general agreement with those reported previously.[2,18] The values for other solvents (DMSO-$d_6$, acetone-$d_6$, $D_2O$ buffer) were in accordance with those obtained in $CDCl_3$ (data deposited as electronic supplementary information†).

### Vicinal coupling constants

To assess the conformational behaviour of the 14-membered macrocycle and two sugar units, oleandrose and desosamine, in compounds **1** and **2**, we measured vicinal proton–proton $^3J_{H,H}$ coupling constants in various solvents as well as carbon–proton $^3J_{C,H}$ coupling constants around the glycosidic bonds. Some homonuclear coupling constants could not be determined even at high temperatures due to severe peak overlapping.

Change of solvent caused major alterations only in $^3J_{H2,H3}$ values (Table 1). Unlike azithromycin,[14] the two compounds failed to demonstrate a recognizable trend in the change of $^3J_{H2,H3}$ coupling constant with the change of solvent polarity. According to $^3J_{H2,H3}$ values (Table 1) the folded-out conformation seems to be predominant for compound **2** in all four solvents. Compound **1** tends to adopt predominantly the folded-out conformation in $D_2O$ buffer, acetone-$d_6$ and $CDCl_3$ and the folded-in conformation in DMSO-$d_6$.

With a mixture of conformers present in solution, a temperature dependence of their relative populations and, accordingly, of the coupling constant values, can be assumed. In both compounds increasing the temperature in DMSO-$d_6$ and buffered $D_2O$ up to 100 °C had an effect only on the value of $^3J_{H2,H3}$ coupling. The coupling constant moderately decreased (Table 2) in buffered $D_2O$ and DMSO-$d_6$ solution for **2** suggesting an increased abundance of the folded-in conformer in the mixture. For compound **1** the $^3J_{H2,H3}$ value did not follow the change in temperature in buffered $D_2O$ (Table 2). This may have been due to the existence of a third stable conformer ($^3J_{H2,H3} \sim 7$ Hz) or to a temperature independent equilibrium between the two conformers. In DMSO-$d_6$, the $^3J_{H2,H3}$ value for **1** was temperature dependent and it increased with increasing temperature (Table 2) suggesting a change of conformation from the folded-in to the folded-out.

**Table 2** Temperature effects on $^3J_{H2,H3}$/Hz in buffered $D_2O$ and DMSO-$d_6$ for compounds **1** and **2**

| | **1** | | **2** | |
|---|---|---|---|---|
| Temperature/°C | DMSO-$d_6$ | $D_2O$ | DMSO-$d_6$ | $D_2O$ |
| 27 | 3.8 | 7.3 | 8.0 | 9.4 |
| 40 | 4.0 | 7.3 | overlap | 9.2 |
| 50 | 4.0 | 7.3 | 7.3 | 9.1 |
| 60 | 4.2 | 7.4 | 7.1 | 8.9 |
| 80 | 4.5 | 7.3 | 6.8 | 8.3 |
| 100 | 4.7 | — | 6.5 | — |

Heteronuclear $^3J_{C,H}$ coupling constants over the glycosidic bonds in **1** and **2** were obtained from multi-site selective one-dimensional experiments using Hadamard formalism[19,20] (Fig. 1). The sensitivity was improved by performing four simultaneous experiments coded according to the Hadamard matrix and later separated by reference to the same matrix. The selective excitation of the macrocycle carbons C3 and C5 and sugar carbons C1′ and C1″ led to the determination of the $^3J_{C,H}$ values listed in Table 3. These are important for identifying the positions and mobility of the sugar moieties with respect to the lactone ring. The values of $^3J_{C,H}$ couplings over the glycosidic bonds in **1** and **2** are within the range of those measured for erythromycin,[21] roxythromycin,[21] clarithromycin[21] and our recently measured data for azithromycin (Table 3), the differences, however, suggest the general conformational flexibility over both glycosidic bonds.

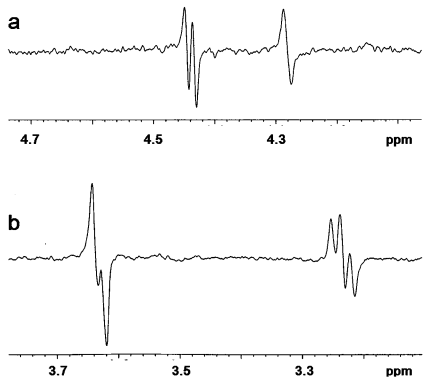


**Fig. 1** Proton spectra of **1** after selective excitation of (a) C5 and (b) C1′ carbons involved in glycosidic linkage according to the Hadamard formalism.

The large diaxial proton–proton coupling constants in the sugar rings are in accordance with the chair conformation of sugar residues.

### Nuclear Overhauser enhancement

Awan *et al.*[11] suggested caution in the use of $^3J_{H2,H3}$ as a sole indicator of the folded-out to folded-in ratio. Further conformational information can be obtained by using the NOE or ROE data. The folded-out and folded-in conformational families are characterized also by a close approach of atoms H3 and H4 to H11 which respectively give rise to H3–H11 NOE peaks in the folded-in and to H4–H11 NOE peaks in the folded-out conformers. The two types of conformer are also reported to be characterized by several other proton–proton spatial proximities such as H5–H18(6Me) for the folded-out and H4–H18(6Me) and H16(2Me)–H17(4Me) for the folded-in conformations.[11]

Therefore, the TPPI NOESY and States-TPPI ROESY spectra for **1** and **2** were recorded and analysed. The NOESY spectra were recorded in $CDCl_3$ solution and the ROESY spectra in DMSO-$d_6$, acetone-$d_6$ and in buffered $D_2O$ (Table 4) because NOEs were close to zero in these solvents at 500 MHz, while ROEs were positive. Features of the NOESY and ROESY spectra of our utmost interest were spatial proton–proton contacts between H3 or H4 on the one side of the ring and H11 on its other side—illustrating the conformation of the macrocycle. Other interesting features were inter-sugar contacts and contacts between sugars and the lactone ring—demostrating the position of the sugar moieties.

A large crosspeak that appeared in the spectrum of **1** between protons H4 and H11 suggested the existence of the folded-out conformer as the predominant one in $CDCl_3$. The peak became weaker in the buffered $D_2O$ solution and in acetone-$d_6$. This effect could be accounted for by an inward folding of the C3–C5 region giving rise to a slight increase in the

**Table 3** Comparison of the vicinal carbon–proton coupling constants ($^3J_{C,H}$/Hz) over the glycosidic bond obtained from the NMR experiment for compounds **1**, **2** and related macrolides[21] and the ones calculated from the X-ray (CSD[7]) torsion angles ($\Phi$/°) for compounds **1a**, **2** and **3** (solution *vs.* solid state conformation)

| Protons | NMR | | | | | | X-Ray (CSD[7]) | | | | | | | |
|---|---|---|---|---|---|---|---|---|---|---|---|---|---|---|
| | **1** | **2** | Erithromycin[21] | Roxithromycin[21] | Clarithromycin[21] | Azithromycin[a] | **1a**[3] | | **2**[6] | | **3**[5] | | | |
| | $^3J_{C,H}$ measured DMSO-$d_6$/$CDCl_3$ | $^3J_{C,H}$ measured $CDCl_3$ | $^3J_{C,H}$ measured $CDCl_3$ | $^3J_{C,H}$ measured $CDCl_3$ | $^3J_{C,H}$ measured $CDCl_3$ | $^3J_{C,H}$ measured $CDCl_3$ | $\Phi$ | $^3J_{C,H}$ calc. | $\Phi$ | $^3J_{C,H}$ calc. | $\Phi$ | $^3J_{C,H}$ calc. | | |
| H3,C1″ | 2.9/5.0 | 5.1 | 4.3 | 5.6 | 5.9 | 2.2 | 28.9 | 3.8 | 19.0 | 4.4 | 17.7 | 4.4 | | |
| C3,H1″ | 5.6/5.5 | 3.3 | 3.6 | 2.0 | 3.5 | 4.1 | 30.5 | 3.7 | 30.5 | 3.7 | 44.0 | 2.6 | | |
| H5,C1′ | 6.3/6.0 | 4.8 | 5.6 | 5.2 | 6.0 | 6.7 | 12.7 | 4.6 | −25.5 | 3.6 | 0.1 | 4.7 | | |
| C5,H1′ | 3.7/3.8 | 3.3 | 2.6 | 5.0 | 3.1 | 3.5 | 51.7 | 2.0 | 34.3 | 3.4 | 41.5 | 2.8 | | |

[a] Unpublished data.

**Table 4** Qualitative nuclear Overhauser enhancement (NOE) data for compounds **1** and **2** in various solvents

| | **1** | | | | **2** | | | |
|---|---|---|---|---|---|---|---|---|
| Proton | $D_2O$ | DMSO-$d_6$ | Acetone-$d_6$ | $CDCl_3$ | $D_2O$ | DMSO-$d_6$ | Acetone-$d_6$ | $CDCl_3$ |
| 2 | 4,4Me | 4,4Me | 4,4Me | 4,4Me | 4Me | 4,4Me | 4,4Me | 4,4Me |
| 3 | 6,5 | 2Me,6,5,11 | 2Me,7a,5 | 2Me,4,5,6 | 2Me,4,6 | 2 or 4Me,6,5 | 2Me,4Me,4,11,5 | 2Me,4,6,11 |
| 4 | | 7b | | | | | | |
| 5 | 6Me | 6Me | 6Me | 6Me,4Me,4 | 6Me,4 | 6Me,4Me | 6Me,4 | 6Me,4Me,4,6 |
| 6 | | 7b | 7b | | | 4 | | |
| 7a | | 4,6,12Me | 4,6,12Me | 4,6,12Me | | 4,6 | 6 | 6 |
| 7b | | 6Me | 6Me | 6Me | | 6Me,6 | 6Me | 6Me |
| 8 | | 7b,6Me,10Me | 10Me,6Me,7b | 6Me,7b,6,10Me | 6Me,6 | 6Me,6,7b,10Me | 6Me,7a,6,10Me | 6Me,6,7b,10Me |
| 10 | 12Me | 12Me,7a,12,8a | 12Me,12,7a | 12Me,12,7a | 12Me,7b | 12Me,7a,12 | 12Me,12,7a,7b | 12Me,7b |
| 11 | 12Me,10,12,4,7a | 12Me,7a,10,12,4 | 10Me,12Me,12,4,11 | 12Me,4,7a,10 | 4,12,10,7a | 4,10,7a | 12Me,12,4,7a,10 | 12Me,10Me,12,4,7a,10 |
| 12 | 13Me | 13Me | 13Me | 10Me,13Me | | 10Me,13Me | 10Me,13Me | 10Me,13Me |
| 13 | 12,11 | 12,11 | | 12,11 | 12,11 | 12,11 | 12,11 | 12,11 |
| 13Me | | | 12Me | | | | | |
| 1′ | 4Me,3′,5″ | 4Me,3′,5,5′,5″ | 4Me,3′,5,5′,5″ | 4Me,3′,5″5,5′ | 4Me,3′,5′,5″ | 4Me,3′,5″,5,5′ | 4Me,3′,5,5′,5″ | 4Me,4′b,5′Me,3,5,5′,5″ |
| 2′ | | 4′a,4′b,3′$NMe_2$ | 4′a,4′b,3′$NMe_2$ | 4′b,3′$NMe_2$ | | 4′b,3′$NMe_2$ | 4′b,3′$NMe_2$ | 4′b,3′$NMe_2$ |
| 3′ | | 4′a,3′$NMe_2$ | 4′a,4′b,3′$NMe_2$ | 4′a,3′$NMe_2$ | 4′a,4′b | 4′a,3′$NMe_2$ | 4′a,4′b,3′$NMe_2$ | 5′Me,4′a |
| 3′$NMe_2$ | | 4′a,4′b | 4′a | 4′a,4′b | | 4′a,4′b | 4′a,4′b | 4′a,4′b |
| 4′a | | 5′Me | 5′Me | | | | | |
| 5′ | 4′a,4′b,3′ | 4′a,4′b,3′ | 4′a,4′b,3′,2′ | 4′a,4′b,3′ | 4′a,4′b | 4′a,4′b,3′ | 4′a,4′b,3′ | 4′a,4′b |
| 1″ | 2Me,2″a,2″b,3 | 4Me,2″a,2″b,3″,3 | 2Me,2″a,2″b,3″,3 | 2Me,2″a,2″b,3 | 2Me,2″a,2″b,3″,5″ | 2Me,2″a,2″b,3,3″,5″ | 2Me,2″a,2″b,3 | 2Me,2″a,2″b,3 |
| 2″a | 2Me | 4Me | 4Me | 2Me | | 4Me | 2Me | 4Me |
| 2″b | | | | | | | | |
| 3″ | 2″a,2″b,4″ | 2″a,4″ | 2″a,2″b,4″ | 2″a,2″b | 2″a,2″b | 2″a,5″Me | 5″Me,4″,2″a,2″b | 5″Me,4″,2″a,2″b |
| 3″OMe | | 2″a | 2″a | 2″a,4″ | 2″a | 2″b | 2″a | 2″a |
| 4″ | 5″Me,2″b | 5″Me,2″b | 5″Me,2″b | 5″Me,2″b | 5″Me,2″b | 5″Me,2″b,2″a | 5″Me,2″a,2″b | 5″Me,2″b |
| 5″ | 4″ | 4″ | 3″ | 4″,3″ | 4″,3″ | 4″,3″ | 4″ | 4″,3″ |

folded-in conformation. The appearance of a ROE crosspeak H3–H11 in DMSO-$d_6$ supported the existence of the folded-in conformation. These findings were consistent with the results of our analysis of the coupling constants. The appearance of the crosspeak H5–H18(6Me) in the ROESY spectra of **1** in all solvents demonstrated that a close approach of H5 and H18(6Me) protons did not characterize only the folded-out conformations as stated previously[11] but the folded-in ones as well. This is in accordance with the available crystal structures of BBOLEA[3] and ZATPAL[6] representing the folded-in and the folded-out conformations of oleandomycin-like compounds, respectively, where H5–H18(6Me) contact was found to be within 2.6 Å for both conformations. Thus we now believe that the H5–H18 contact can not be taken as evidence for the folded-out conformation since it has been observed for both folded-in and folded-out conformers of oleandomycin and azithromycin.

In the spectra of compound **2**, the H4–H11 ROE crosspeak was relatively strong in $D_2O$ buffer and DMSO-$d_6$ (Fig. 2) and somewhat weaker in $CDCl_3$ and acetone-$d_6$ where a weak H3–H11 peak also appeared (Table 3). This, along with our data concerning the coupling constants, provided support for the conclusion that compound **2** existed predominantly in the folded-out conformation in solution with some contribution of the folded-in conformer especially in acetone and $CDCl_3$.

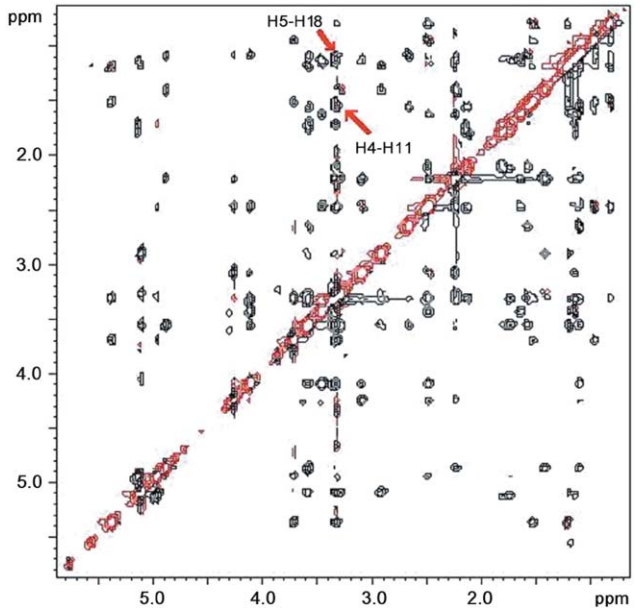


**Fig. 2** States-TPPI ROESY NMR spectrum of **2** in DMSO-$d_6$ solution at 27 °C. The key NOE crosspeaks are marked.

The NOE and ROE data for **1** and **2** show the expected crosspeaks for sugars in the Everett–Tyler[8] chair conformation except for $D_2O$ where, owing to the poor quality of spectra, some contacts could not be identified. This conformation was characterized by H1′–H3′, H1′–H5′, H3′–H5′ and H2′–H4′(a,b) NOE crosspeaks for the chair conformation of the desosamine unit and by H2″(a,b)–H4″ and H4″–H6″(5″Me) for the chair of oleandrose sugar.

Two contacts between the macrocycle and desosamine were observed in **1** and **2**: H5–H1′ and H17(4Me)–H1′. They corresponded to the perpendicular orientation of desosamine with respect to the lactone ring and agreed with the data reported for the related macrolides.[8–15] Contacts between the macrocycle and oleandrose such as H3–H1″ and inter-sugar contact H1′–H5′ indicated an oleandrose position similar to that of cladinose in clarithromycin.[13] For both compounds a characteristic macrocycle–oleandrose contact H16(2Me)–H1″ ROE was found in all solvents. The only exception was the DMSO solution of **1** where the H17(4Me)–H1″ crosspeak was observed instead, as a consequence of a larger proportion of the folded-in conformer. Namely, in the folded-in conformation the H17(4Me) group was closer to cladinose/oleandrose giving rise to a H17(4Me)–H1″ ROE contact.

## Molecular modelling

Incorporation of the experimental NMR constraints into modelling simulations did not seem to be the right approach as it could yield an average conformation that never actually existed. Therefore, independent unconstrained molecular dynamics simulations were performed and molecular modelling focused on the 3D structural interpretation of the NMR experimental findings. In the molecular regions not covered by the NMR data *i.e.* C8–C9–O9/N9–OH and O14–C1–O1 modelling results were indispensable for deducing conformation. Solvents for simulations were chosen according to the changes of interest in the NMR data that we wanted to account for conformationally.

The NMR coupling constants and torsion angles obtained by modelling were compared by means of the Karplus-type equation (see Experimental). Due caution was exercized considering the parameterization of the equation and tolerance of agreement between the couplings and torsions.

The NMR NOE data were the second check point for simulation results—sampled conformations were checked for the existence of NOEs found by NMR.

**Conformation of the macrocycle.** After the molecular mechanics energy minimization of compound **1** (Scheme 1), performed using the Consistence Valence Force Field (cvff) in Discover,[22] the initial folded-in conformation (Tables 5 and 6, conformation IN for **1a** X-ray) was retained (Tables 5 and 6, conformation $IN_2$ for **1** Modelling). Molecular dynamics (MD) simulations were performed in DMSO using the cvff in Discover.[22] Two protocols were employed, one at the constant temperature of 300 K and the other at 300 K with temperature jumps to 500 K. During simulations changes in the C–C–C–C and corresponding H–C–C–H torsion angle values on the right-hand side of the macrocycle became apparent and approximately two groups of different values, corresponding to two different conformational families, could be distinguished (Tables 5 and 6). The torsions on the left-hand side of the macrocycle were more or less unchanged. The folded-in conformational family (torsion angle H2–C2–C3–H3 ~ 100°) was the more densely populated one during simulations, but the folded-out conformers (torsion angle H2–C2–C3–H3 ~ ±180°) could also be seen (Fig. 3a). The folded-out conformers were more abundant in the simulation with temperature jumps. The change in torsion angle values was accompanied by a change in characteristic inter-proton contacts (Fig. 3b). The difference in energy between the folded-in and folded-out conformational families was within 1.5 kcal $mol^{-1}$.

During the molecular dynamics simulations in $H_2O$ for **1** (data not shown) the folded-in conformation was no longer the more densely populated one; the folded-in and folded-out conformers of the 14-membered macrocycle were found to co-exist in a mixture.

A superposition diagram of the folded-in and folded-out conformers from MD simulations in DMSO for **1** and of the folded-in solid-state conformer for **1a**[3] is shown in Fig. 4.

After the molecular mechanics energy minimization for compound **2**, performed using cvff in Discover,[22] the initial folded-out conformation (Tables 5 and 6, conformation OUT for **2** X-ray) was retained (Tables 5 and 6, conformation $OUT_{Ins.}$ for **2** Modelling). In molecular dynamics trajectories in $CDCl_3$ and $H_2O$ at 300 K the conformations positioned mainly around the starting folded-out molecular mechanics energy minimum were observed again (Fig. 3c and d). That meant that the average simulation value of $^3J_{H2,H3}$ was larger than its experimental NMR value. The folded-in conformation, with small $^3J_{H2,H3}$ coupling which would lower the average trajectory value, although expected, failed to appear during simulation even after temperature jumps to 500 K. Likewise,

**Table 5** Selected torsion angles H–C–C–H ($\Phi$/°) calculated from NMR $^3J_{H,H}$ data (Table 1) and the ones obtained by modelling calculations for selected folded-in and folded-out conformers of **1** and **2** in comparison with the solid state X-ray conformers of oleandomycin derivatives[3,5,6] retrieved from CSD[7]

| | **1** | | | | | | | | **2** | | | | | | | | **1a**[3] | **2**[6] | **3**[5] |
|---|---|---|---|---|---|---|---|---|---|---|---|---|---|---|---|---|---|---|---|
| | NMR | | | | Modelling | | | | NMR | | | | Modelling | | | | X-Ray (CSD[7]) | | |
| | $D_2O$ | DMSO | Acetone | $CDCl_3$ | DMSO | | | | $D_2O$ | DMSO | Acetone | $CDCl_3$ | $CDCl_3$ | | | | Solid state | | |
| Torsion angle | OUT + IN | IN | OUT + IN | OUT + IN | $IN_1$ | $IN_2$ | $OUT_1$ | $OUT_2$ | OUT + IN | OUT + IN | OUT + IN | OUT + IN | $OUT_{Ins.}$ | $OUT_{Syb.}$ | $IN_{Ins.}$ | $IN_{Syb.}$ | IN | OUT | "OUT" |
| H2–C2–C3–H3 | 136.1 | 117.1 | 131.6 | 142.6 | 88.4 | 95.0 | 165.0 | 172.6 | 149.2 | 140.1 | 134.4 | 139.5 | 172.2 | 151.4 | 109.0 | 101.9 | 115.3 | 169.8 | −179.4 |
| H3–C3–C4–H4 | −62.9 | −62.9 | −63.9 | — | −63.5 | −66.1 | −72.7 | −75.9 | −65.0 | −68.7 | −61.9 | −68.7 | −73.8 | −75.6 | −65.4 | −61.8 | −65.4 | −74.6 | −82.8 |
| H4–C4–C5–H5 | 137.3 | — | 135.5 | 136.1 | 176.9 | 164.7 | 152.9 | 129.9 | 157.8 | 159.0 | 153.9 | 164.6 | 160.5 | 158.7 | 174.0 | 179.2 | 162.1 | 155.6 | 154.3 |
| H5–C5–C6–H6 | −61.9 | — | −60.0 | −58.2 | −63.5 | −64.1 | −85.5 | −74.3 | — | — | −95.7 | — | −93.4 | −77.1 | −67.2 | −64.1 | −74.0 | −98.5 | −72.9 |
| H6–C6–C7–H7a | — | — | — | — | −67.3 | −65.8 | −72.0 | −71.6 | — | — | — | — | −73.3 | −64.7 | −70.8 | −61.3 | −54.1 | −62.5 | −67.0 |
| H6–C6–C7–H7b | — | — | −150.8 | −137.6 | 179.4 | −179.3 | 175.6 | 175.6 | 150.7 | 150.7 | — | 153.5 | 176.4 | −179.4 | 177.4 | −176.2 | −174.1 | 177.5 | 175.3 |
| H10–C10–C11–H11 | 65.1 | 58.5 | 59.5 | 65.1 | 65.5 | 64.4 | 71.4 | 69.8 | 71.2 | 65.1 | 63.9 | 65.1 | 65.1 | 72.0 | 62.4 | 71.4 | 68.1 | 66.7 | 60.7 |
| H11–C11–C12–H12 | 167.1 | 164.5 | 159.2 | 174.8 | 178.8 | 176.2 | 179.6 | 178.9 | 172.2 | — | — | 170.0 | 176.5 | 174.8 | 175.2 | 164.0 | 173.3 | 176.2 | 172.0 |
| H12–C12–C13–H13 | −64.4 | −58.6 | −60.4 | −65.6 | −59.8 | −61.6 | −64.4 | −66.7 | −68.1 | −69.6 | −65.6 | −66.8 | −65.9 | −63.7 | −73.5 | −63.9 | −57.9 | −66.2 | −84.6 |

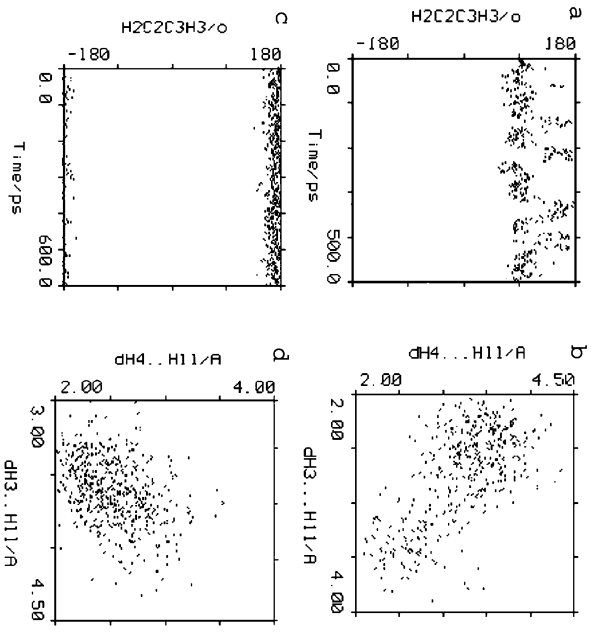


**Fig. 3** Trajectory of H2–C2–C3–H3 torsion angle and H3–H11 *vs.* H4–H11 distances from MD simulation in DMSO at 300 K for **1** (a, b) and from MD simulation in $H_2O$ at 300 K with jumps to 500 K for **2** (c, d). Changes from predominantly folded-in (torsion angle H2–C2–C3–H3 ~ 90°, contact H3···H11) to folded-out conformation (torsion angle H2–C2–C3–H3 ~ 170°, contact H4···H11) can be seen for **1**. No conformational changes are observed for **2**; the folded-out conformation was maintained throughout simulation.

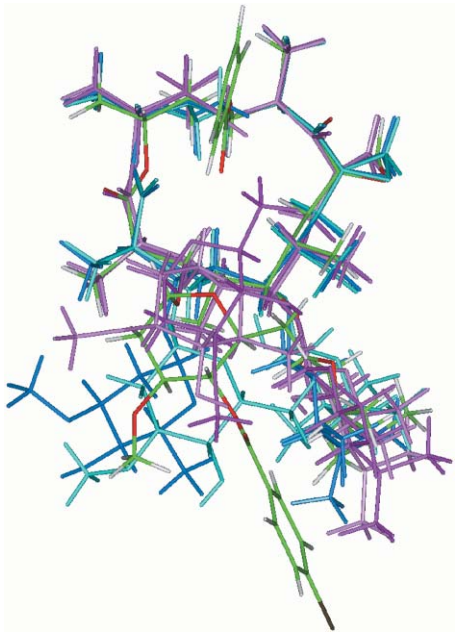

**Fig. 4** Superposition diagram of the folded-in (light and dark pink; Table 6 conformations $IN_1$ and $IN_2$) and folded-out (light and dark turquoise; Table 6 conformations $OUT_1$ and $OUT_2$) conformers of **1** modelled by Insight II[22] and folded-in X-ray[3] conformer of **1a** (coloured by atom; Table 6 conformation IN). Atoms of the macrocycle were used for superposition.

molecular dynamics simulations at higher temperature (500 K) failed to confirm the existence of such a conformation, although other conformations appeared but were abandoned not being in accordance with the NMR data.

In the attempt to assess the folded-in conformer of **2** a change of force field seemed appropriate. Molecular mechanics energy minimization performed on **2** in Sybyl[23] using the MMFF94 force field revealed a change in conformation from the initial folded-out (Tables 5 and 6, conformation OUT for **2** X-ray) to the folded-in (Tables 5 and 6, conformation $IN_{Syb.}$ for **2** Modelling). The folded-in conformer so obtained was reoptimized again in Discover[22] using cvff (Tables 5 and 6, conformer $IN_{Ins.}$ for **2** Modelling) and had an energy exceeding that of a previous folded-out conformer by ~ 5 kcal mol$^{-1}$. In Sybyl[23] the situation was different: energetically, the folded-in conformer was the more favoured one. The reoptimized folded-in conformer from Discover[22] was then used as a starting

**Table 6** Selected torsion angles C/O–C–C–C/O/N ($\Phi$/°) for folded-in and folded-out conformers of **1** and **2** obtained by modelling calculations in comparison with the torsion angles of the solid state X-ray conformers of oleandomycin derivatives[3,5,6] retrieved from CSD[7]

| | **1** | | | | **2** | | | | **1a**[3] | **2**[6] | **3**[3] |
|---|---|---|---|---|---|---|---|---|---|---|---|
| | Modelling (MD, DMSO) | | | | Modelling (MD, $CDCl_3$) | | | | X-Ray (CSD[7]) | | |
| Torsion angle | $IN_1$ | $IN_2$ | $OUT_1$ | $OUT_2$ | $OUT_{Ins.}$ | $OUT_{Syb.}$ | $IN_{Ins.}$ | $IN_{Syb.}$ | IN | OUT | "OUT" |
| O14–C1–C2–C3 | 107.6 | 97.0 | 110.3 | 119.3 | 106.4 | 117.4 | 125.6 | 81.5 | 83.8 | 109.4 | 122.0 |
| C1–C2–C3–C4 | −142.9 | −135.9 | −72.7 | −66.3 | −65.5 | −86.5 | −121.4 | −130.5 | −119.3 | −67.0 | −60.2 |
| C2–C3–C4–C5 | 169.9 | 169.0 | 162.7 | 158.0 | 160.7 | 162.9 | 170.4 | 177.4 | 175.2 | 162.2 | 153.3 |
| C3–C4–C5–C6 | −59.3 | −70.8 | −82.9 | −102.8 | −75.6 | −79.6 | −63.2 | −61.4 | −75.9 | −83.7 | −83.3 |
| C4–C5–C6–C7 | −64.8 | −65.7 | −87.5 | −76.2 | −96.1 | −78.7 | −71.2 | −64.3 | −72.4 | −90.0 | −73.1 |
| C5–C6–C7–C8 | 173.4 | 174.3 | 169.7 | 169.0 | 170.9 | 179.3 | 174.2 | −178.0 | −171.8 | 177.7 | 171.5 |
| C6–C7–C8–C9 | −57.6 | −52.1 | −67.9 | −63.2 | −95.7 | −74.2 | −97.2 | −78.0 | −65.4 | −77.9 | −163.2 |
| C7–C8–C9–C10 | −85.5 | −83.0 | −63.2 | −68.7 | −23.7 | −63.3 | −37.1 | −68.9 | −69.9 | −49.9 | 43.4 |
| C8–C9–C10–C11 | 100.1 | 98.2 | 106.3 | 105.7 | 92.8 | 105.6 | 104.0 | 106.6 | 107.3 | 103.8 | 49.6 |
| C9–C10–C11–C12 | −169.2 | −170.8 | −163.1 | −164.9 | −172.6 | −166.3 | −176.4 | −167.0 | −171.3 | −170.2 | −171.5 |
| C10–C11–C12–C13 | −178.1 | 179.6 | −177.3 | −177.9 | −179.0 | 180.0 | 179.3 | 170.0 | 176.0 | −178.2 | 168.7 |
| C11–C12–C13–O14 | −63.7 | −64.5 | −69.7 | −72.3 | −73.3 | −68.4 | −81.1 | −65.7 | −72.4 | −68.4 | −88.7 |
| C12–C13–O14–C1 | 117.8 | 134.3 | 96.7 | 97.5 | 96.7 | 100.4 | 97.2 | 145.4 | 154.2 | 98.4 | 104.9 |
| C13–O14–C1–C2 | −160.4 | −161.3 | 179.6 | 180.0 | −179.4 | 177.7 | −151.7 | −173.1 | −174.4 | 173.2 | 173.3 |
| C13–O14–C1–O1 | 17.2 | 16.5 | −0.9 | −0.5 | −1.0 | −1.7 | 27.0 | 5.8 | 5.0 | −6.7 | −5.8 |
| C3–C2–C1–O1 | −70.1 | −80.8 | −69.3 | −60.3 | −72.0 | −63.3 | −53.1 | 97.4 | −95.6 | −70.6 | −58.9 |
| C7–C8–C9–O9/N9 | 92.6 | 94.8 | 115.2 | 109.5 | 156.4 | 116.6 | 145 | 110.8 | 123.1 | 131.7 | −134.0 |
| C11–C10–C9–O9/N9 | −77.9 | −79.5 | −72.0 | −72.4 | −87.3 | −74.3 | −77.9 | −73.1 | −85.4 | −77.6 | −132.7 |
| C8–C9–N9–O91 | — | — | — | — | −19.8 | −1.4 | −16.1 | −0.2 | — | −3.5 | 2.0 |
| C10–C9–N9–O91 | — | — | — | — | 160.3 | 178.5 | 165.8 | 179.6 | — | 178.1 | −175.6 |
| C9–N9–O91–H91 | — | — | — | — | 177.8 | −179.6 | 178.1 | −179.8 | — | 175.7 | 161.1 |
| C2–C3–O3–C1″ | −109.2 | −75.1 | −99.3 | −129.4 | −105.5 | −100.9 | −82.5 | −81.5 | −90.4 | −103.4 | −101.8 |
| C4–C3–O3–C1″ | 120.3 | 156.0 | 134.1 | 104.3 | 148.9 | 137.0 | 151.3 | 154.7 | 148.8 | 135.0 | 137.3 |
| C3–O3–C1″–C2″ | 133.8 | −175.4 | 149.2 | 103.2 | 148.9 | 146.8 | 155.8 | 158.3 | 151.9 | 150.5 | 164.6 |
| C3–O3–C1″–O5″ | −104.9 | −52.1 | −87.6 | −135.3 | −87.8 | −89.9 | −80.3 | −77.7 | −89.8 | −85.6 | −73.5 |
| C4–C5–O5–C1′ | −109.5 | −106.0 | −111.6 | −100.0 | −120.5 | −113.8 | −109.0 | −110.6 | 109.9 | −144.5 | −117.8 |
| C6–C5–O5–C1′ | 122.1 | 124.9 | 121.9 | 132.7 | 114.7 | 122.6 | 122.9 | 124.1 | 130.5 | 92.8 | 118.9 |
| C5–O5–C1′–C2′ | 167.9 | 179.0 | 163.5 | 174.4 | 165.5 | 166.9 | 172.4 | 173.4 | 171.1 | 154.3 | 161.6 |
| C5–O5–C1′–O5′ | −71.6 | −60.2 | −76.2 | −65.2 | −74.0 | −73.0 | −66.6 | −66.4 | −66.6 | −86.4 | −77.7 |

point for new molecular dynamics simulation in Discover[22] in $CDCl_3$. To start from different conformations in order to better sample the conformational space seemed more advantageous than to run a very long molecular dynamics at low sampling efficiency. The folded-in conformation, however, changed almost immediately to the folded-out conformation.

During the molecular dynamics simulation in Discover[22] the E ↔ Z isomerization of the oxime chain occurred for the double bond C8–C9=N9–OH. This isomerization was probably due to a weak force constant for the C8–C9=N9–OH torsion angle calculated by automatic parameter assignment. According to synthesis[2] and X-ray data,[6] only the conformers with the C8–C9=N9–O torsion angle of ~0° were considered, isomerization in the solution being highly improbable.

Fig. 5 shows a superposition diagram of the folded-out and folded-in conformers of **2** from MD simulations in $CDCl_3$ in Discover[22] and Sybyl[23] as well as the folded-out solid-state conformer.[6]

On the whole, conformational changes had influenced three groups of torsions at the right-hand side of the macrocycle: (a) C1–C2–C3–C4 and H2–C2–C3–H3 angles, (b) C3–C4–C5–C6 and H4–C4–C5–H5 angles, and (c) C4–C5–C6–C7 and H5–C5–C6–H6 angles (Tables 5 and 6; Fig. 4 and 5). The change (a) in torsion angles could be clearly observed from the NMR data (change in $^3J_{H2,H3}$) while the other two torsion angle changes [(b) and (c)], due to their lesser extent, could not be easily recognized in the NMR data. The torsion angles at the left-hand side of the macrocycle were more or less unaffected.

The changes in torsion angles were accompanied by changes of intra-macrocycle proton to proton distances: H3,H4–H11 but also H6–H10,H11 and H7–H10,H11—the larger values being characteristic of the folded-in and the smaller ones of the folded-out conformers. All distances were within 5 Å.

Further conformational flexibility, independent of the folded-in ↔ folded-out transformation, was noticed in the regions C7–C8–C9(O9/N9–OH)–C10 and C12–C13–O14–C1=O1 where different types of conformation were recognized (Table 6, Fig. 4 and 5). Comparable conformational changes were reported for clarithromycin by Steinmetz *et al.*[12] (flexibility of the lactone region) and for roxithromycin by Gharbi-Benarous *et al.*[24] who attributed them to hydrogen bonding. We also noticed different types of intramolecular hydrogen bonding (O11—H···O1=C1, O11–H···N9/O9=C9, O11–H···O91–N9=C9 and C9=N9–O91–H···O11) during the MD simulations but did not find their link with the conformation to be conclusive. In the solid-state folded-out conformer of **2** the presence of the hydrogen bond O11–H···O1=C1 was registered while in the solid-state folded-in conformer of **1a** there was no possibility of hydrogen bonding as the hydroxyl group at C11 was benzylated.

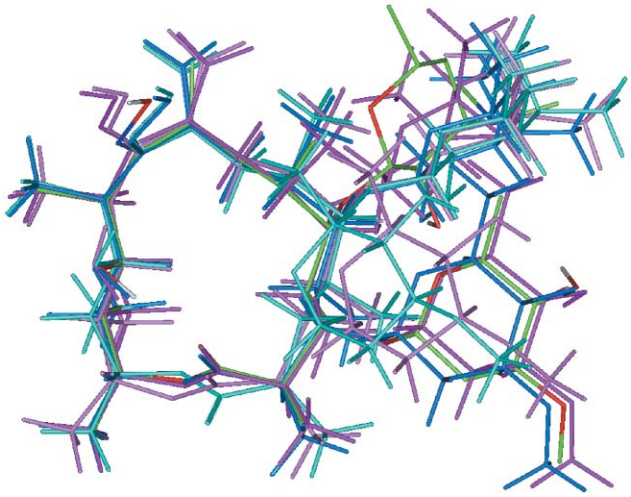

**Fig. 5** Superposition diagram of the different conformers of **2**: folded-out (dark pink; Table 6 conformation $OUT_{Ins.}$) and folded-in (light pink; Table 6 conformation $IN_{Ins.}$) conformers from modelling in Insight II,[22] folded-out (dark turquoise; Table 6 conformation $OUT_{Syb.}$) and folded-in (light turquoise; Table 6 conformation $IN_{Syb.}$) conformers from modelling in Sybyl[23] and folded-out X-ray[6] conformer (coloured by atom; Table 6 conformation OUT). Formation of the hydrogen bond O11–H···O=C1 in folded-out conformers can be observed. Atoms of the macrocycle were used for superposition.

**Conformation of the sugar rings and conformation around the glycosidic bond.** During all MD simulations the oleandrose and desosamine sugar moieties kept the usual and expected chair conformation in both compounds—β-$^4C_1$ for desosamine and α-$^1C_4$ for oleandrose. The conformational behaviour of the glycosidic bond was comparable for the two compounds (**1** and **2**; Fig. 6). The conformational family around the X-ray conformer was the most densely populated one; the formation of another family conformationally close to the X-ray conformer could be noticed especially for compound **2** (Fig. 6c and d). With the latter compound the second conformational family seemed to be populated independently of the simulation temperature whereas in the case of **1** its population density was much lower even in simulations with temperature jumps. After the molecular mechanics energy minimization of the selected MD conformers, the conformation around the glycosidic bond of the desosamine sugar residue usually adopted conformations close to the solid-state conformer both for **1** and **2** while a few different conformations around the glycosidic bond of oleandrose proved to be stable (Table 6). In all conformers the oleandrose sugar moiety held a coplanar position towards the macrocycle and the desosamine sugar moiety a perpendicular one (Fig. 4 and 5). As molecular dynamics data revealed a certain conformational flexibility and did not support a single conformational model around the glycosidic bond, it was concluded that only conformational averaging could yield good agreement between theoretical modelling and experimental NMR results. Thus, NMR parameters were found to reflect an average conformation and to suggest that solution conformation was a mixture of different conformations which could not be adequately described solely by the crystal structure conformation.

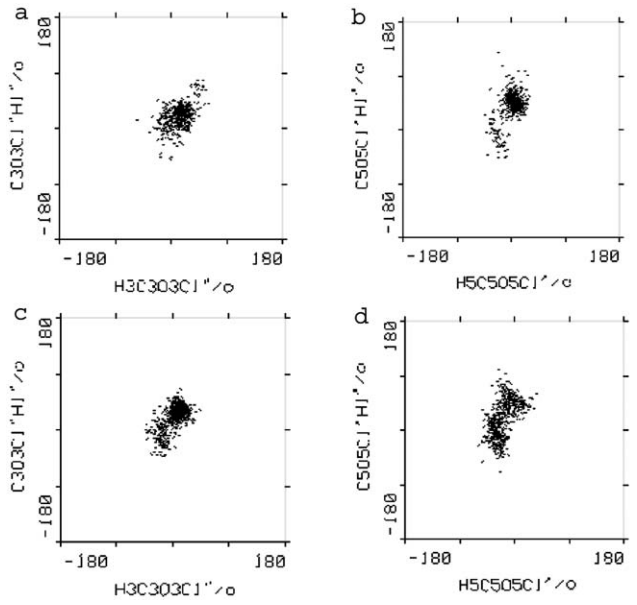


**Fig. 6** Conformation around the glycosidic bond defined by torsion angles H5–C5–O5–C1′ and C5–O5–C1′–H1′ for the desosamine sugar moiety and by H3–C3–O3–C1″ and C3–O3–C1″–H1″ for oleandrose during the MD simulation in DMSO at 300 K for **1** (a, b) and in $H_2O$ at 300 K with jumps to 500 K for **2** (c, d).

## Conclusions

A combined use of NMR spectroscopy and molecular modelling has provided insight into the conformational properties of oleandomycin **1** and its 8-methylene-9-oxime derivative **2**.

Oleandomycin **1** adopts predominantly the folded-in conformation in DMSO. A small amount of the folded-out conformation present increases upon heating ($^3J_{H2,H3}$ rises and the abundance of folded-out conformer in molecular dynamics trajectory grows with the temperature). A mixture of the folded-in and folded-out conformers exists in buffered $D_2O$, acetone-$d_6$ and $CDCl_3$.

Conformational analysis for compound **2** shows the folded-out conformation to be the preferred one in all solvents (although some amounts of the folded-in conformer can also be present depending on the solvent and the temperature) and in the solid state.[6]

For both compounds molecular modelling has also revealed conformational flexibility in the regions around C1 and C9, which are not covered by the NMR data. It is assumed that intramolecular hydrogen bonding can have some influence on the conformation of the macrocycle, particularly on the conformation in those regions, but the evidence has not been conclusive.

The large diaxial coupling constants and characteristic NOE crosspeaks in the sugar rings as well as modelling results have provided evidence that both sugars tend to adopt the usual chair conformation characteristic also of the solid state, oleandrose being coplanar and desosamine perpendicular to the lactone ring. Both glycosidic bonds exhibit a certain conformational flexibility around the X-ray conformer.

Our results have demonstrated that the measured NMR parameters tend to reflect an average, virtual conformation and that the X-ray structures do not adequately describe solution state conformations. Compounds **1** and **2** exhibited conformational flexibility not only in the erythronolide part but also in the position of sugar rings. Bearing in mind the knowledge gained from this study, once different conformations have been modelled, in further conformational studies of the oleandomycin-type compounds the coupling constants $^3J_{H2,H3}$, especially their temperature dependence, and the NOE proton–proton distances H3–H11 and H4–H11 can serve as good indicators of the aglycone ring folding.

## Experimental

### NMR Spectroscopy

One and two-dimensional NMR spectra were recorded on a Bruker Avance DRX500 spectrometer equipped with a 5 mm diameter inverse detection probe and z-gradient accessory working at 500.13 MHz for $^1$H. In $^1$H NMR experiments the spectral width was 5000 Hz, the number of data points 65K and the number of scans 8–64. TMS was used as the internal standard. The sample concentration was 10 mg mL$^{-1}$ in $CDCl_3$, acetone-$d_6$ and DMSO-$d_6$ solutions and 2 mg mL$^{-1}$ in 50 mM $D_2O$ phosphate buffer (pH = 7.6) solution. Pulse scheme WATERGATE (3–9–19) was used for the water signal suppression. The digital resolution was 0.1 Hz per point.

Two-dimensional gsCOSY, ROESY and NOESY spectra were recorded under the following conditions: spectral width was 6000 Hz in both dimensions, 2K data points were applied in time domain and 512 increments were collected for each data set with linear prediction to 1K and zero filling to 2K. Scans 4–32 were applied for each increment. The relaxation delay was 1.5 s. States-TPPI ROESY spectra were obtained with the mixing time of 250 ms (400 ms for NOESY) and processed with a sine squared function shifted by π/2 in both domains, while gsCOSY spectra were processed with an unshifted sine function. The digital resolution was 2.7 and 10.7 Hz per point in f2 and f1 domains, respectively.

The HSQC and HMBC spectra were recorded with a relaxation delay of 1.5 s and 32 scans per increment. The spectral width was 31000 Hz in acquisition domain f2 and 6000 Hz in time domain f1. Data were collected into a 2048 × 256 acquisition matrix and processed using a 2K × 1K transformed matrix with zero filling in the f1 domain. Sine multiplication was performed before Fourier transformations. In HMBC spectra the delay for long-range couplings was set to 60 ms.

Measurements of long-range $^{13}C$–$^{1}H$ couplings were performed using the multiple $^{13}C$ site selective excitation experiment[19,20] on a Varian Unity Inova 600 spectrometer operating at 600.07 MHz for protons with an inverse detection gradient probe. Half-Gaussian shaped pulse truncated at the leading edge at 5% maximum intensity was used for selective $^{13}C$ excitation with a duration of 25–50 ms. The relative sign of each selective pulse was set according to the Hadamard matrix. Spectral widths of 4000–5000 Hz were sampled with 32768 data points using 5000 scans for each Hadamard excitation. A BIRD module was used for a better selection of long-range couplings. The two gradients were applied before and after the last pair of 90° pulses for coherence selection and suppression of artefacts.

### Molecular modelling

The coordinates from X-ray analysis, taken from the Cambridge Structural Database[7] (CSD), were used as a starting point for calculations. For compound **1** the coordinates from **1a**[3] (Scheme 1) were taken. The *p*-bromobenzoyl substituents were replaced by hydroxyl groups in the Builder module of the Insight II program[22] (Accelrys). Hydrogen atoms were added according to the stereochemistry in the Builder module of the Insight II program.[22] For compound **2** the starting coordinates were also taken from CSD[7] (Scheme 1); the coordinates for the hydroxyl hydrogens of **2** were provided by the author[6] and others were generated on the basis of stereochemistry again in the Builder module of the Insight II program.[22]

The molecular mechanics energy minimizations were performed using cvff in the Discover module of the Insight II program.[22] The atomic potentials and charges were assigned in cvff. For comparison some calculations were performed using Merck Molecular Force Field (MMFF94) and MMFF94 charges in the Sybyl package[23] (Tripos).

Molecular dynamics simulations were carried out with cvff in the Discover module of the Insight II program.[22] As the input for simulations, sterically relaxed X-ray structures were taken. The molecules were placed in a cubic box, which was subsequently filled with solvent molecules. Explicit solvent molecules (non-continuum solvation model) were used in order to take into account solvation effects, which is not possible in a homogeneous dielectric environment. Simulations were performed using periodic boundary conditions (PBC) with the minimum image model. Before they started, an energy minimization was performed on the whole system. Simulations were carried out in $H_2O$ for both compounds, in DMSO[25] for **1** and in $CDCl_3$ for **2**. The solvents for simulations were chosen according to the effects of interest in the NMR data. For the simulations in $CDCl_3$ and DMSO it was first necessary to adjust the density to an appropriate value for each solvent, using pNT conditions. The molecular dynamics simulations were then performed at constant volume and at 300 K, by coupling to a thermal bath, during 500 ps with the step of 1 fs preceded by an equilibration period of 50 ps. In some simulations brief temperature jumps to 500 K were performed in order to prevent staying in the same local energy gap and to help jumping over possible higher energy barriers by increasing the kinetic energy and enabling, in that way, a change of conformation. These simulations lasted for 600 ps. For compound **2**, in the attempt to provoke conformational changes, MD simulations at 500 K were also performed. No constraints were applied. The coordinates were sampled every 100 steps.

The NMR coupling constants $^{3}J_{H,H}$ were transformed to torsion angle values, and *vice versa*, using the Karplus-type equation by Hasnoot *et al.*[26] modified according to the electronegativity and orientation of the substituents by an in-house program based on graphic interpolation. For $^{3}J_{C,H}$ couplings over the glycosidic bond the equation by Tvaroška and Gajdoš[27] was used.

All calculations were performed using PLIVA's Indigo² SGI workstation and the Octane SGI workstation of the Ruer Bošković Institute, Zagreb, Croatia.

## Acknowledgements

Thanks from Zrinka Banić Tomišić are due to Dr. Biserka Kojić Prodić, Head, Laboratory for Chemical and Biological Crystallography, Ruer Bošković Institute, Zagreb, Croatia for the use of hardware and software facilities.

## References

1 F. A. Hochstein, H. Els, W. D. Celmer, B. L. Shapiro and R. B. Woodward, *J. Am. Chem. Soc.*, 1960, **82**, 3225.
2 G. Lazarevski, G. Kobrehel, S. okić, L. Kolačny-Babić, B. Kojić-Prodić, D. Janković and V. Puntarec, *J. Antibiot.*, 1994, **47**, 349.
3 H. Ogura, K. Furuhata, Y. Harada and Y. Iitaka, *J. Am. Chem. Soc.*, 1978, **100**, 6733; CSD refcode: BBOLEA.
4 G. M. Bright, A. R. English, A. A. Nagel, J. A. Retsema and F. C. Sciavolino, *Antimicrob. Agents Chemother.*, 1984, **25**, 113.
5 G. Lazarevski, G. Kobrehel, S. okić and L. Kolačny-Babić, *J. Antibiot.*, 1994, **47**, 349; CSD refcode: LIDBIJ.
6 B. Kamenar, N. Košutić Hulita, I. Vicković and G. Lazarevski, *Z. Kristallogr.*, 1995, **210**, 516; CSD refcode: ZATPAL.
7 F. H. Allen and O. Kennard, *Chem. Des. Automat. News*, 1993, **8**, 31.
8 J. R. Everett and J. W. Tyler, *J. Chem. Soc., Perkin Trans. 2*, 1987, 1659.
9 J. Gharbi-Benarous, P. Ladam, M. Delaforge and J.-P. Girault, *J. Chem. Soc., Perkin Trans. 2*, 1993, 2303.
10 A. Awan, R. J. Brennan, A. C. Regan and J. Barber, *J. Chem. Soc., Chem. Commun.*, 1995, 1653.
11 A. Awan, R. J. Brennan, A. C. Regan and J. Barber, *J. Chem. Soc., Perkin Trans. 2*, 2000, 1645.
12 W. E. Steinmetz, R. Bersch, J. Towson and D. Pesiri, *J. Med. Chem.*, 1992, **35**, 4842.
13 W. E. Steinmetz, J. D. Sadowsky, J. S. Rice, J. J. Roberts and Y. K. Bui, , *Magn. Reson. Chem.*, 2001, **39**, 163.
14 G. Lazarevski, M. Vinković, G. Kobrehel, S. okić, B. Metelko and D. Vikić-Topić, *Tetrahedron*, 1993, **49**, 721.
15 N. Košutić-Hulita, D. Matak-Vinković, M. Vinkovic, P. Novak, G. Kobrehel and G. Lazarevski, *Croat. Chem. Acta*, 2001, **74**, 327.
16 F. Schlünzen, R. Zarivach, J. Harm, A. Bashan, A. Tocilj, R. Albrecht, A. Yonath and F. Franceschi, *Nature*, 2001, **413**, 814.
17 J. L. Hansen, J. A. Ippolito, N. Ban, P. Nissen, P. B. Moore and T. A. Steitz, *Mol. Cell*, 2002, **10**, 117.
18 A. A. Nagel, W. D. Celmer, M. T. Jefferson, L. A. Vincent, E. B. Whipple and G. Schutle, *J. Org. Chem.*, 1986, **51**, 5397.
19 E. Kupče and R. Freeman, *J. Magn. Reson., Ser. A*, 1993, **105**, 310.
20 V. Blechta, F. Rio-Portillas and R. Freeman, *Magn. Reson. Chem.*, 1994, **32**, 134.
21 G. Bertho, P. Ladam, J. Gharbi-Benarous, M. Delaforge and J-P. Girault, *Int. J. Biol. Macromol.*, 1998, **22**, 103.
22 Insight II release v. 2000 (modules: Builder, Discover v. 2.98, Analysis), 2002, Accelrys Inc., Paris, France.
23 Sybyl v. 6.8, 2002, Tripos Inc., München, Germany.
24 J. Gharbi-Benarous, P. Ladan, M. Delaforge and J. P. Girault, *J. Chem. Soc., Perkin Trans. 2*, 1992, 1989.
25 D. F. Mierke and H. Kessler, *J. Am. Chem. Soc.*, 1991, **113**, 9466.
26 C. A. G. Haasnot, F. A. A. M. de Leeuw and C. Altona, *Tetrahedron*, 1980, **36**, 2783.
27 I. Tvaroška and J. Gajdoš, *Carbohydr. Res.*, 1995, **271**, 151.